Chapter 7

The Autonomous Flight

Tone Magister and Franc Željko Županič

Additional information is available at the end of the chapter

http://dx.doi.org/10.5772/46484

1. Introduction

The Autonomous Flight Airspace (AFA) [9] is the evolutional offspring of the Free Flight Airspace (FFA), and enabler of integrated flight operations of aircraft with autonomous flight capabilities (for instance, Unmanned Aircraft Systems (UAS)).

In the FFA the responsibilities for the airborne spacing and separation assurance are delegated to flight crews on board the aircraft, and the ground–based Air Traffic Management (ATM) is to resume separation authority in emergencies only [2]. Therefore, humans are the decision–makers, as well as operatives in the FFA.

Since airborne separation assurance is a fundamental principle of the FFA and the Airborne Separation Assurance System (ASAS) its main enabler, the AFA introduces the autonomous airborne separation assurance with Autonomous–ASAS (AASAS). The AFA is marked by the machine–based decision–making, and the AFA is restricted to the ASAS and AASAS equipped aircraft but both types with autonomous flight capabilities. In the future the only humans–in–the–loop conducting flight operations through AFA are going to be ground–based UAS operators, air traffic flow managers of the next generation ATM, and systems supervisors (*pilots of present–day terminology*) onboard remnant "old–school" manned aircraft. Based on 4D trajectory planning the AASAS concept covers machine–based (a) traffic situational awareness, and (b) airborne spacing and self–separation assurance through (c) autonomous in–flight conflict detection and resolution.

The AFA concept is not only important for implementation of non–segregated UAS flight operations [8], but also for the future air transport system responding to the society's emerging needs (which are not limited to enabling permeability of increasing volume of air traffic, but include other issues; i.e., for example airborne security when it is necessary for the pilot to transfer his/her responsibilities to an automatic system due to a hijack situation for flight trajectory protection and safe automatic return to the ground as envisioned in [1]).

Analogous to the traffic complexity at both highway ends, air traffic is inherently complex especially in both zones adjacent to the boundary between the AFA (or FFA) and non–autonomous (or un–free) flight airspace (non–AFA). The number (quantum) of conflicts between aircraft is proportional to the complexity of the in–flight traffic situation [7]. For AFA implementation (or any airspace organization with changing delegation of responsibilities for the airborne spacing and separation assurance), the transition flights between the AFA and non–AFA therefore represent a critical safety issue.

The prediction accuracy of the future trajectory of each and every aircraft aloft drive the stability of the predicted four-dimensional traffic situation in the airspace confined with a look-ahead time and consequently the ASAS and/or AASAS on-board each aircraft ability to detect every potential conflicton-time and correctly. The statement holds for either free-flight [2], sector-less airspace [4], or automated airspace [5] envisioned to cope with the increasing demand in the crowded skies above.

With the existing technology and methodology the look-ahead time for the construction of accurate future aircraft flight trajectory is reduced to only about 5 to 7 minutes in advance. Prolonged look-ahead timeusing the current airborne separation assurance technology, designed not to include the future intent,results in predicted traffic situation instability [6] and consequently in conflict detection unreliability or even inability.

The study is also focused on the design of an advanced four-dimensionalmodel of aircraft relative flightproviding the capabilities of the AASAS to detect conflicts beyond the borders of the AFA and enabling Autonomous Flight concept implementation.

2. Autonomous flight airspace

2.1. Problem of transition flight to/from autonomous flight airspace

The complexity of air traffic and quantum of in–flight conflicts between aircraft in the AFA (or FFA) and its non–AFA neighborhood can be investigated using the theory of airspace fractal dimensions proposed by Mondoloni and Liang in [11]. This theory was introduced as methodology capable of simultaneously distinguishing between complexity of air traffic situation as a consequence of management of air traffic flow, and complexity of an air traffic situation as a consequence of geometry and organization of airspace. Fractal dimension is a number $D \in \{D \in \mathbb{R}, 1 \le D \le 3\}$ assigned to the particular flight corresponding to freedom of aircraft motion. As shown in Table 1, with increasing freedom of movement the fractal dimension of flight increases, and vice versa.

The frequency of in–flight conflicts decreases exponentially if fractal dimension of aircraft flight increases. Alternatively, the number of in–flight conflict encounters C threatening aircraft ($dC = CR\,dt$) increases with decreasing freedom of its flight ΔD, and their relation can be approximated from data of Table 1 as:

$$\int CR\,dt \approx 11.472 - 2.452\Delta D \tag{1}$$

Scenario / Degrees of Freedom				Fractal Dimension
Airway Network	Heading	Airspeed	Top of Descent	
D	D	D	D	1.0
D	n/a	**F**	n/a	2.0
e	**F**	D	n/a	2.0
e	**F**	n/a	D	2.0
n/a	D	**F**	**F**	2.1
e	**F**	n/a	**F**	2.4
e	**F**	**F**	n/a	2.6
Controlled Airspace / Transition Areas *form 10,000ft to FL410; 120nm box around airport*				1.22 – 1.39
Upper Control Area *upper airspace above FL240*				1.13 – 1.32
TMA/CTA – Terminal and Control Area *from 10,000ft to FL240*				1.2

D Determined parameter
F Free parameter
e Exclusive parameter
n/a Undefined parameter

Table 1. The fractal dimension of flight is proportional to the freedom of movement (data compiled from [11]).

Since descending and/or climbing aircraft through the sector of level cruising flights markedly increase the air traffic controller's workload [3], and consequently decrease sector throughput, earlier studies such as [2] anticipated mostly level transition flights from the FFA (and applicable to the AFA as well). Level transition flights to and from the AFA (or FFA) require that the AFA (or FFA) and the controlled airspace (CA) are positioned side by side. Such airspace configuration again increases the air traffic controller's workload by introducing the mix of differently equipped aircraft subjected to essentially different procedures, namely the mix of controlled flights and autonomous (or free) flights en–route to or from the AFA (or FFA). However, to simultaneously gain increased airspace capacity and flight economics together with decreased emissions from optimized flights, the AFA (or FFA) should and will extend above CA (Fig. 1). Obviously there is more than one reason to consider transition to and from the AFA (or FFA) while aircraft are climbing or descending.

The transition flight from the AFA into the CA results in significantly decreased freedom of flight; aircraft path might be dictated directly by ATM or at least to a certain extent confined by the route network. Due to decrease in freedom of flight the fractal dimension of aircraft path will decrease (Table 1) and consequently the in–flight conflict encounter for transitioning aircraft will inevitability increase (1). The greater the differences between fractal dimensions of flight in the AFA and CA are, the greater is the increase in conflict encounter for transitioning aircraft at the boundary between the AFA and CA.

The greatest (50%) decrease of fractal dimension of flight and resulting drastic 135% increase of conflict encounters (1) occurs, when an aircraft transits the border between the AFA (or

FFA) and the CA through the arbitrary place (TC) at level flight and enters directly into the network of airways of CA.

The solution to the problem of transition flight conflict encounter increase at the border between the AFA (or FFA) and the CA consists of:

1. the transition to and from the AFA (or FFA) into the CA in non–level flight; i.e., introduction of transition in descent and climb;
2. gradually decreased degree of freedom of flight in the direction from the AFA (or FFA) into the CA; i.e., progressively dictated parameters of flight along the transitioning route before an aircraft leaves the AFA (or FFA), upon leaving the AFA, and afterwards while flying in the CA (and vice versa for the flight in the opposite direction transitioning to the AFA (or FFA));
3. CA organization and air traffic flow regulation adequate to the procedures of autonomously (or free) flying aircraft entering from the AFA (or FFA) and mixing with the rest of the traffic.

The proposed solution to the transitioning flight problem is presented in Fig. 1. Drastic increase in conflict encounter imminent to an aircraft at the AFA border in level transition flight is dispersed. In consequence, severity of conflict encounters along its transitioning trajectory is reduced.

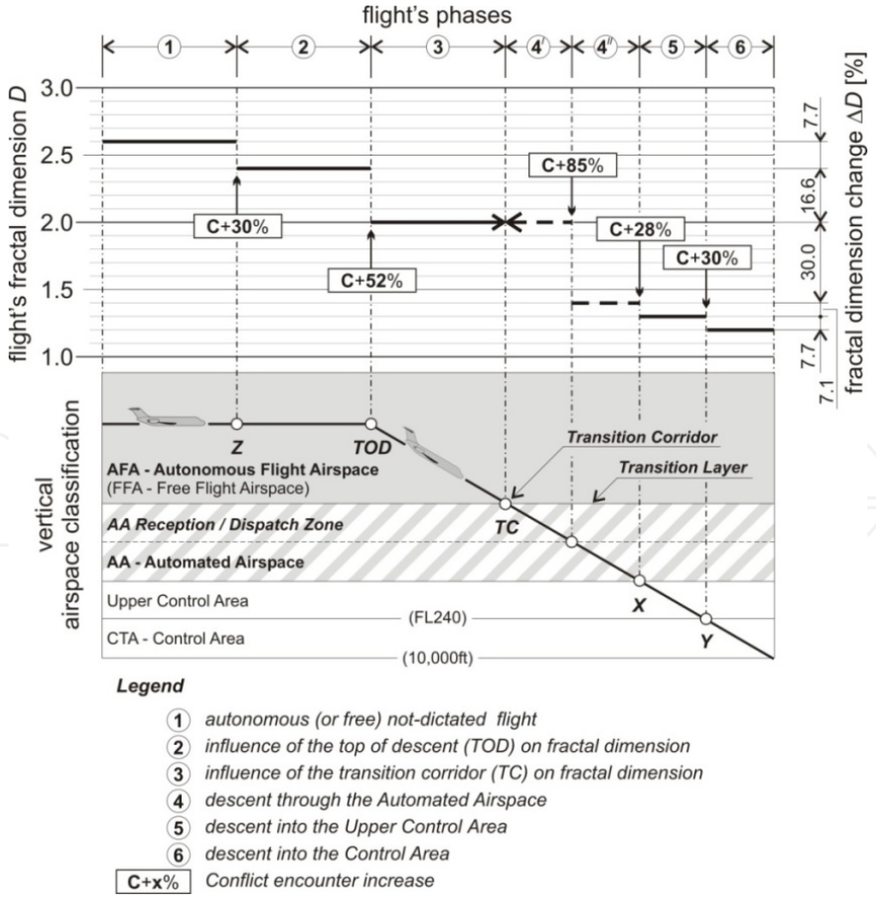

Figure 1. Conflict increase dispersion along descending transition from the AFA.

The top of descent (TOD) determination in the AFA has a two–fold impact on the freedom of flight decrease while an aircraft is still flying in the AFA. Determination of the TOD in the AFA itself (Table 1), as the trajectory determination factor, reduces the fractal dimension of flight even before an aircraft reaches the edge of the AFA (Z; Fig. 1). Furthermore the TOD can only be determined by the intersection of an aircraft cruising level and the trajectory of its descent (with a constant rate of descent to the assigned destination) through the rest of the transitioning aircraft free transition corridor (TC; Fig. 1) closest to the optimal route through the border between the AFA and CA. The transition corridor (TC) is a one–way passage in the transition layer through which an aircraft flies from the AFA into the CA (and vice versa); at the same time it is the starting point of a particular airway in the CA. The TC defines the four–dimensional position of an aircraft transitioning from the AFA and direction of flight in the CA adjacent to the transition layer; consequently the TC is the restrictive factor which decreases freedom of aircraft movement and the fractal dimension of its flight (Table 1). Recurrently determined TOD and TC define the route of an aircraft leaving the AFA, and by gradually decreasing its freedom of flight dispersing threatening conflict encounters with neighboring aircraft along its way.

Descending from the AFA via the TC an aircraft enters the CA. In the part of the CA that borders upon the AFA it is of a critical importance that the autonomous flights can be safely integrated with the rest of not–autonomous traffic, and that the airspace organization including traffic flow management enables a fractal dimension comparable to the fractal dimension of the AFA. Both major criteria of the CA bordering the AFA are met with the Automated Airspace (AA) type of CA proposed in [4], if a reception zone is introduced into the AA at its border with the AFA.

The AA is based upon the ground–based automation system that provides in–flight separation assurance via data–link communication for properly equipped aircraft. The ground–based automation system issue clearances for aircraft intended trajectories and/or it can up–load safe trajectories directly into the flight management system module of the AASAS of the autonomous aircraft and ASAS of the non–autonomous aircraft.

The roles of controllers in the AA are strategic control of traffic flow, handling of unusual traffic situations, and monitoring and control of unequipped aircraft [4]. This facilitates the autonomous and non–autonomous aircraft mix in the AA.

The reception zone is an integral part of the AA adjacent to the border with the AFA (flying in the opposite direction an aircraft leaves the AA through the dispatch zone). The concourse pattern of airways starting in the AA reception zone with each TC at the border with the AFA is adjusted to match the directions of cardinal routes of the AFA; their geometry and organization serves as a collector of air traffic flows from various TCs onto the main central airways of the AA. The airways structure and management of traffic flow--i.e., the aircraft trajectory control and restrictions--are such that the fractal dimension of the AA reception zone corresponds to the AFA fractal dimension. The fractal dimension of a flight upon crossing the border between the AFA and AA reception zone remains unchanged allowing that in the most critical part of the transition flight in the vicinity of the

TC and in the TC the conflict encounter does not increase for the transitioning aircraft (Fig. 1).

Descending through the CA below the AA the aircraft traverse airspace sectors of different classes with progressively increased restrictions and control (dictation) of its trajectory each time the sector boundary is crossed, leading to non–severe but gradual increase in conflicts in succession of each sector boundary crossing (X,Y; Fig. 1). However the greatest fractal dimension of a non–AA CA is far less than the AA reception zone fractal dimension. Consequently the greatest (30%) change of fractal dimension of a transitioning flight is expected to occur in the AA resulting in an 85% increase in conflict encounter (1) threatening descending aircraft (Fig. 1).

The challenge of the AA organization and traffic flow regulation is to progressively dictate the flight of the transitioning aircraft to secure gradual decrease in AA fractal dimension in the direction away from the transition layer from the value corresponding to the AFA fractal dimension with a value similar to the upper CA fractal dimension. That way the expected increase in conflict is dispersed further along the entire descending trajectory through the AA. The spacing and separation assurance actors in the AA are the AASAS of the autonomous aircraft, the ASAS of a free–flying aircraft, crews of unequipped aircraft, the ground–based separation assurance automation system, and the AA strategic traffic flow controller; but parallel to the human error hazard, a data–link communication failure imposes the greatest risk for flight safety in the AA.

2.2. Autonomous flight airspace design

For the safety of aircraft flying in the AFA and AA, both are demarcated by the transition layer (TL), defined by the entry and exit plane that are separated at least by the vertical separation minimum. The AFA extends above the entry plane, while the AA is positioned below the exit plane (Fig. 2). Aircraft are transitioning to and from the AFA through the bordered tube–like transition corridor (TC) at the TL.

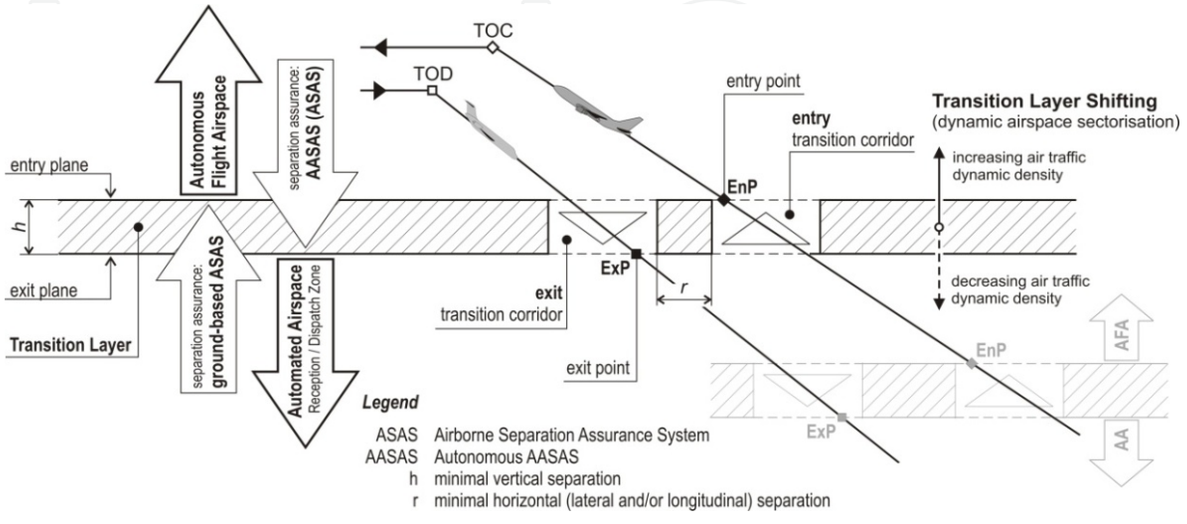

Figure 2. The transition layer between the AFA and the AA.

Aircraft flows from either side of the TL converging for transit through the TCs, leading to the traffic dynamic density increase on either side of the TL in its proximity (applying the WJHTC/Titan Systems Metric: the convergence recognition index, separation critically index, and degrees of freedom index will be the most critical [7]). Traditionally the traffic dynamic density is limited by the air traffic controller workload, however even in the AFA or AA the dynamic density will still remain limiting factor due to the limited airborne and ground–based separation assurance system processor capacity as well as limited data–link bandwidth. Dynamic airspace sectorization will ensure that the air traffic dynamic density doesn't reach its limits by the TL shifting. The (pressure) altitude of the TL is proportional to the air traffic dynamic density trend; if it is increasing, for example, the TL will ascend, resulting in AA vertical expansion simultaneously with the AFA *contraction* (Fig. 2).

In the AFA and AA aircraft, in–flight spacing and separation relies on the machine–based decision–making ASAS; in the AFA the AASAS, responsibility extends to the exit plane of the TL, while in the AA the ground–based automation ASAS responsibilities extend to the entry plane of the TL. Since the exit plane doesn't coincide with the entry plane the airborne spacing and separation of aircraft responsibilities are shared in the TL between the AASAS onboard autonomous aircraft and the ground–based automation ASAS of the AA. Due to shared responsibilities for airborne separation the entrance and exit TCs must be separated; aircraft are flying from the AFA through the exit TC, while they are entering the AFA through the entry TC (Fig. 2). Consequently, and considering again the fact that airborne separation is based upon the machine–based decision–making in the AFA and AA, any conflict avoidance maneuvering can only be coordinated implicitly between the AASAS and/or ASAS onboard aircraft involved in the conflict encounter, including implicit coordination of future 4D trajectories of aircraft in the area.

Since AASAS of autonomously flying aircraft is still responsible for the in–flight spacing and separation when the transitioning aircraft is in the TC at the exit plane of the TL, the AASAS has to be capable of detecting possible conflict situations with aircraft flying in the AA even before the time of transition from the AFA. Actually the rest of the transitioning aircraft-free--and especially conflict-free--exit TC can only be selected (determined) in the process of aircraft descent trajectory from the AFA definition before the TOD is reached, providing that accurate prediction of along the descending route and across the TL airborne traffic situation can be made. The greater look–ahead time for accurate and stable 4D prediction of an airborne traffic situation, demands an accurate model of aircraft future relative positions based on their real future ground speeds, their future intents, as well as on future area weather conditions. (Similar requirements are applicable for the ground–based ASAS of the AA since it is responsible for airborne aircraft spacing and separation in the TC at the entry plane of TL.)

Rules–of–the–sky tailored to the AFA flight operations are necessary for competitive rivalry for the best optimal trajectory prevention, and also due to the fact that conflict avoidance maneuvering can only be coordinated implicitly between AASAS and/or ASAS onboard aircraft. For the transition flight to and from the AFA safety, a pair of rules applies. *The priority flight (first) rule*: "An aircraft that flies lower than the other aircraft involved in the

conflict encounter when conflict is detected, has the right–of–way." The rule therefore implies that only the higher flying aircraft is responsible for resolving the conflict situation. Since the AFA extends above the AA, the autonomous aircraft flying in the AFA are obliged to maneuver for menacing conflict resolution in case they are encountering conflict with an aircraft climbing to enter the AFA from the AA, and in their envisioned descent transition from the AFA. This priority rule also defines minimum separation between the entry and exit plane, as well as minimum separation between the entry and exit TCs at the TL for unnecessary aircraft maneuvering in the AFA prevention. *A maneuver flight (second) rule*: "After a conflict is detected, it is prohibited for the aircraft which has the right–of–way to alter planned trajectory until conflict is resolved." A pair of rules is therefore defined to ensure reliable implicit coordination of conflict avoidance maneuvering and increase conflict resolution predictability.

3. Autonomous airborne separation assurance

3.1. Aircraft relative flight model

The primitive flight model predicts each aircraft's future trajectory with extrapolation of its ground speed vector from aircraft's last position, while the aircraft's ground speed vector is derived with interpolation between its last two known positions. The predictions of this model are therefore based upon a set of presumptions of: (a) constant aircraft ground speed and direction, followed by (b) constant wind speed and direction, and (c) constant static state (temperature) of atmosphere as well.

Let's investigate the reliability of conflict detection in the encounter situation between our own aircraft denoted by index 2 in descent and the intruder denoted by index 1 in level flight below. If the time of the present level cruise phase of own flight is denoted as τ, while t denotes the time of own aircraft descent as a subsequent phase of its flight, then the primitive model of relative position between own aircraft and intruder with the top of descent accounted for as a future intent can be written as:

$$\begin{aligned} \dot{x}_R(\tau,t) &= v_{2G}\cos\psi_R - v_{1G} \\ \dot{y}_R(\tau,t) &= v_{2G}\sin\psi_R \\ \dot{z}_R(\tau,t) &= -v_{2G}\tan\theta_R(\tau,t) \end{aligned} \tag{2}$$

where ψ_R and θ_R are the relative angles between aircraft trajectories in the horizontal and vertical plane successively, and v_G is their ground speed.

Closer examination of a primitive model (2) reveals that, if there is no distinction made between the time of own aircraft level flight and the time of its descent then, the primitive model cannot predict when this aircraft will alter its trajectory. Furthermore, following presumptions of the primitive model described above it is obvious that, even if deficiency of this primitive model is corrected with introduction of each aircraft future intent, this primitive model cannot account for the future aircraft trajectory variations due to the true airspeed variableness as a function of a non-zero vertical static temperature gradient in the troposphere.

The improved model of aircraft flight was derived to include not only the aircraft (crew) future intent but also to consider:

a. the aircraft true airspeed v variableness $v = v(\vartheta_S(z))$ as a function of static state of an atmosphere ϑ_S(i.e. static air temperature (SAT)T; $\vartheta_S(z) = \{T(z)\}$) variation with aircraft height z above reference,
b. the aircraft true airspeed variableness $v = v(\sigma(z))$ due to the changing set of speed regimes $\sigma(z) = \{M, v_C\}$ of descent and/or climb with constant Mach number M and/or with constant calibrated airspeed v_C,
c. the influence of the dynamic state of an atmosphere $\vartheta_D(z) = \{w(z), \xi(z)\}$ defined with the wind speed w and direction ξ on the progressive speed V of an aircraft which can be written as $V = V(v, \vartheta_D(z))$.

Based on the simplification that an angular velocity vector of each aircraft equals to zero, and an assumption that an alteration of each aircraft trajectory is instantaneous (chapter 3.2.1), the improved model of aircraft relative motion is defined with:

$$\begin{aligned} x_R^{/} &= V_2(v_2(\sigma_2(z), \vartheta_S(z)), \vartheta_D(z)) \cos\theta_R(\sigma_2(z)) \cos\psi_R - \\ &\quad - V_1(v_1(\sigma_1(z), \vartheta_S(z)), \vartheta_D(z)) \\ y_R^{/} &= V_2(v_2(\sigma_2(z), \vartheta_S(z)), \vartheta_D(z)) \sin\theta_R(\sigma_2(z)) \cos\psi_R \\ z_R^{/} &= V_2(v_2(\sigma_2(z), \vartheta_S(z)), \vartheta_D(z)) \sin\theta_R(\sigma_2(z)) \end{aligned} \tag{3}$$

andcan be transformed into the time dependant function using the rate of climb (+) or descent (–) definition:

$$\pm\frac{dz}{dt} = V(z) \sin\theta_R(\sigma_2(z)) \tag{4}$$

where the progressive speed V of an aircraft follows form the aircraft speed vector triangle:

$$V(z) = \frac{w\cos(\xi - \psi) + \sqrt{v^2(\sigma(z), \vartheta_S(z)) - w^2 \sin^2(\xi - \psi)}}{\cos\theta_R(\sigma_2(z))} \tag{5}$$

The solution of the improved kinematical model of aircraft relative flight (3; (4) and (5)) is presented, as improved model of the aircraft relative motion, for the case that aircraft abbreviated as A2 and its flight parameters denoted by index 2, starts its descent at the top of descent (TOD) from a cruise level z_{FL2} in stratosphere $z_{FL2} > z_{tp}$ (tropopause at z_{tp}) at $t_{TOD} > t_0$ after conflict is detected at t_0, while the intruder denoted by index 1 continues its constant Mach number M level cruise. The solution of (3) provided is partitioned according to descending aircraft flight phases; note that s, c and t denote trigonometric functions of sine, cosine and tangent.

a. $t_0 \le t \le t_{TOD}$ ($t_0 = 0$): the A2 is in a $M_2 = const$ level cruise ($\theta_2 = 0$) in the stratosphere:

$$
\begin{aligned}
x_R(t) &= x_R(t_0) + \left(w\left(\mathrm{c}_{\lambda_2}\mathrm{c}_{\psi_R} - \mathrm{c}_{\lambda_1} \right) - \sqrt{M_1^2 a_{FL1}^2 - w^2 \mathrm{s}_{\lambda_1}^2} + \mathrm{c}_{\psi_R} \sqrt{M_2^2 a_{tp}^2 - w^2 \mathrm{s}_{\lambda_2}^2} \right) t \\
y_R(t) &= y_R(t_0) + \mathrm{s}_{\psi_R} \left(w\,\mathrm{c}_{\lambda_2} + \sqrt{M_2^2 a_{tp}^2 - w^2 \mathrm{s}_{\lambda_2}^2} \right) t \\
z_R(t) &= z_R(t_0)
\end{aligned}
\tag{6}
$$

where $\mathrm{r}_R(t_0) = (x_R(t_0), y_R(t_0), z_R(t_0))$ is the initial aircraft relative position when conflict is detected at t_0.

b. $t_{TOD} < t \le t_{tp}$: the A2 descends in constant M speed–regime with constant angle of descent $\theta_R = \theta_2$ through the stratosphere:

$$
\begin{aligned}
x_R(t) &= x_R(t_{TOD}) + \left(w\left(\mathrm{c}_{\lambda_2}\mathrm{c}_{\psi_R} - \mathrm{c}_{\lambda_1} \right) - \sqrt{M_1^2 a_{FL1}^2 - w^2 \mathrm{s}_{\lambda_1}^2} + \mathrm{c}_{\psi_R} \sqrt{M_2^2 a_{tp}^2 - w^2 \mathrm{s}_{\lambda_2}^2} \right) t \\
y_R(t) &= y_R(t_{TOD}) + \mathrm{s}_{\psi_R} \left(w\,\mathrm{c}_{\lambda_2} + \sqrt{M_2^2 a_{tp}^2 - w^2 \mathrm{s}_{\lambda_2}^2} \right) t \\
z_R(t) &= z_R(t_{TOD}) - \mathrm{t}_{\theta_2} \left(w\,\mathrm{c}_{\lambda_2} + \sqrt{M_2^2 a_{tp}^2 - w^2 \mathrm{s}_{\lambda_2}^2} \right) t
\end{aligned}
\tag{7}
$$

where $\mathrm{r}_R(t_{TOD})$ is solution of (6) for $t = t_{TOD}$.

c. $t_{tp} < t \le t_p$: after passing the tropopause at t_{tp} the A2 descends in constant M speed–regime through the troposphere:

$$
\begin{aligned}
x_R(t) &= x_R(t_{tp}) + \left[w\left(\mathrm{c}_{\lambda_2}\mathrm{c}_{\psi_R} - \mathrm{c}_{\lambda_1} \right) + \mathrm{c}_{\psi_R} k_5 M_2 \sqrt{\chi R} - \sqrt{M_1^2 a_{FL1}^2 - w^2 \mathrm{s}_{\lambda_1}^2} \right] \left(t - t_{tp} \right) + \mathrm{c}_{\psi_R} k_6 M_2 \sqrt{\chi R} \left(t^2 - t_{tp}^2 \right) \\
y_R(t) &= y_R(t_{tp}) + \mathrm{s}_{\psi_R} \left(t - t_{tp} \right) \left(w\,\mathrm{c}_{\lambda_2} + k_5 M_2 \sqrt{\chi R} \right) + \mathrm{s}_{\psi_R} k_6 M_2 \sqrt{\chi R} \left(t^2 - t_{tp}^2 \right) \\
z_R(t) &= z_R(t_{tp}) - \mathrm{t}_{\theta_2} \left(t - t_{tp} \right) \left(w\,\mathrm{c}_{\lambda_2} + k_5 M_2 \sqrt{\chi R} \right) - \mathrm{t}_{\theta_2} k_6 M_2 \sqrt{\chi R} \left(t^2 - t_{tp}^2 \right),
\end{aligned}
\tag{8}
$$

where $\mathrm{r}_R(t_{tp})$ is solution of (7) for $t = t_{tp}$, while k_5, k_6, and k_1 and k_2 are:

$$
k_5 = \sqrt{T_{0R} + \frac{L}{2k_2} \left[k_1 - \sqrt{k_1^2 + 4k_2 \left(t_{tp}\mathrm{t}_{\theta_2} + z_{tp} \left(k_1 + k_2 z_{tp} \right) \right)} \right] - \frac{w^2 \mathrm{s}_{\lambda_2}^2}{M_2^2 \chi R}}
\tag{9}
$$

$$
k_6 = L\,\mathrm{t}_{\theta_2} \left(4k_5 \sqrt{k_1^2 + 4k_2 \left(t_{tp}\mathrm{t}_{\theta_2} + z_{tp} \left(k_1 + k_2 z_{tp} \right) \right)} \right)^{-1}
\tag{10}
$$

$$
k_1 = \left(w\,\mathrm{c}_{\lambda} + \sqrt{M^2 \chi R T_{0R} - w^2 \mathrm{s}_{\lambda}^2} \right)^{-1}
\tag{11}
$$

$$
k_2 = \frac{k_1^2 ML \sqrt{\chi R}}{4} \left(T_{0R} - \frac{w^2 \mathrm{s}_{\lambda}^2}{M^2 \chi R} \right)^{-\frac{1}{2}}
\tag{12}
$$

d. $t > t_p$: at t_p the A2 changes its speed–regime and continues its descent through the troposphere with the constant calibrated airspeed ($v_{C2} = const$):

$$
\begin{aligned}
x_R(t) &= x_R(t_p) + \left[w\left(\mathrm{c}_{\lambda_2}\mathrm{c}_{\psi_R} - \mathrm{c}_{\lambda_1} \right) + \mathrm{c}_{\psi_R} k_7 - \sqrt{M_1^2 a_{FL1}^2 - w^2 \mathrm{s}_{\lambda_1}^2} \right]\left(t - t_p \right) + \mathrm{c}_{\psi_R} k_8 \left(t^2 - t_p^2 \right) \\
y_R(t) &= y_R(t_p) + \mathrm{s}_{\psi_R}\left(t - t_p \right)\left(w\,\mathrm{c}_{\lambda_2} + k_7 \right) + \mathrm{s}_{\psi_R} k_8 \left(t^2 - t_p^2 \right) \\
z_R(t) &= z_R(t_p) - \mathrm{t}_{\theta_2}\left(t - t_p \right)\left(w\,\mathrm{c}_{\lambda_2} + k_7 \right) - \mathrm{t}_{\theta_2} k_8 \left(t^2 - t_p^2 \right),
\end{aligned}
\tag{13}
$$

where $r_R(t_p)$ is solution of (8) for $t = t_p$, while k_7, k_8, k_9, k_{10}, and k_3, k_4 are:

$$
k_7 = \sqrt{\frac{2\chi R T_{0R}}{\chi - 1}\left(1 + \frac{L k_9}{2 k_4 T_{0R}} \right)\left[\left(k_{10}\left(1 + \frac{L k_9}{2 k_4 T_{0R}} \right)^{-\frac{g_0}{LR}} + 1 \right)^{\frac{\chi - 1}{\chi}} - 1 \right]} - w^2 s_{\lambda_2}^2 \tag{14}
$$

$$
k_8 = \frac{\chi R L \mathrm{t}_{\theta_2}}{2\left(\chi - 1 \right)\left(k_3 - k_9 \right) k_7}\left[-1 + \left(k_{10}\left(1 + \frac{L k_9}{2 k_4 T_{0R}} \right)^{-\frac{g_0}{LR}} + 1 \right)^{\frac{\chi - 1}{\chi}}\left(1 - \frac{\left(\chi - 1 \right) g_0 k_{10}}{\chi R L}\left(k_{10} + \left(1 + \frac{L k_9}{2 k_4 T_{0R}} \right)^{\frac{g_0}{LR}} \right)^{-1} \right) \right] \tag{15}
$$

$$
k_9 = k_3 - \sqrt{k_3^2 + 4 k_4 \left(\mathrm{t}_{\theta_2} t_p + z_p\left(k_3 + k_4 z_p \right) \right)} \tag{16}
$$

$$
k_{10} = \left(1 + \frac{\chi - 1}{2}\left(\frac{v_{C2}}{a_0} \right)^2 \right)^{\frac{\chi}{\chi - 1}} - 1 \tag{17}
$$

$$
k_3 = \left(w\,\mathrm{c}_{\lambda} + \sqrt{\frac{v_C^2 T_{0R}}{T_0} - w^2 \mathrm{s}_{\lambda}^2} \right)^{-1} \tag{18}
$$

$$
k_4 = \frac{k_3^2}{4}\left(\frac{v_C^2 T_{0R}}{T_0} - w^2 \mathrm{s}_{\lambda}^2 \right)^{-\frac{1}{2}}\left(\frac{v_C^2 L}{T_0} - 2 g_0\left(1 + \frac{\chi - 1}{2}\left(\frac{v_C}{a_0} \right)^2 \right)\left[1 - \left(1 + \frac{\chi - 1}{2}\left(\frac{v_C}{a_0} \right)^2 \right)^{-\frac{\chi}{\chi - 1}} \right] \right) \tag{19}
$$

The abbreviations not given in the text are: g_0 is acceleration of gravity, L is (temperature atmospheric) lapse rate, R is universal gas constant, χ is ratio of specific heats, a_0 and a_{FL} are speed of sound at reference level of standard atmosphere and at aircraft flight level (FL), T_0 and T_{0R} are reference SATs of standard and real atmosphere, λ represents the difference between the wind direction ξ and aircraft true heading ψ, while index R denotes the relative parameter.

3.2. Accuracy of modeling

3.2.1. Simplifications based errors

At the top of descent (TOD) an aircraft starts its rotation $\boldsymbol{\Omega}(t)=(0,\omega_\theta,0)$ (for $t\in[0,t_t]$) about its lateral axis until the angle of descent θ is established after transition time t_t as is shown in Fig. 3.

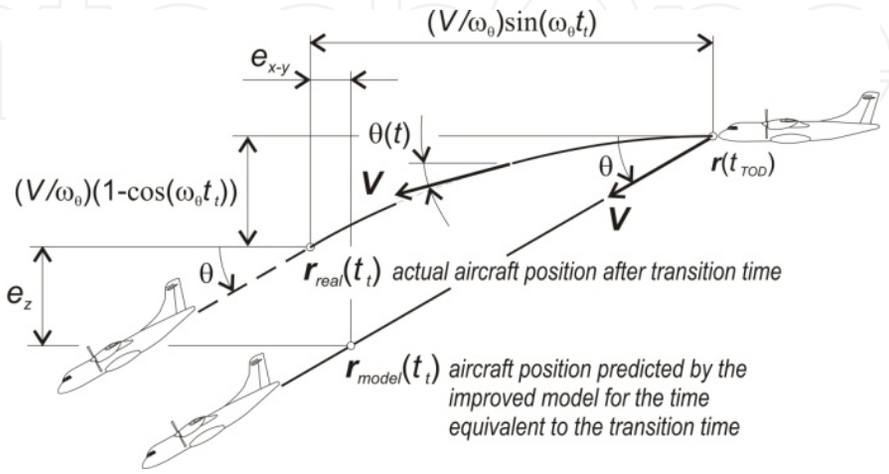

Figure 3. Simplified transition into descent.

For simplicity of an improved model of aircraft relative flight (3) the instantaneous aircraft transition into descent is assumed:

$$\lim_{t_t\to 0}\frac{V}{\omega_\theta}\left(1-\cos\left(\omega_\theta t_t\right)\right)=0$$
$$\lim_{t_t\to 0}\frac{V}{\omega_\theta}\sin\left(\omega_\theta t_t\right)=0 \tag{20}$$

Due to simplification (20), the aircraft trajectory is not smooth at the TOD, resulting in the horizontal e_{x-y} and vertical e_z plane error of aircraft position prediction in the period of transition time $t\in[0,t_t]$ .It can be theoretically estimated from Fig. 1 as:

$$e_{x-y}(t_t)=V(t_t)\left(\cos\theta-\frac{\sin\theta}{\hat{\theta}}\right)t_t$$
$$e_z(t_t)=V(t_t)\left(\sin\theta-\frac{1-\cos\theta}{\hat{\theta}}\right)t_t \tag{21}$$

The position errors e_{x-y} and e_z (21) are proportional to the transition time t_t, angle of descent θ, and aircraft progressive speed $V=f(v(\sigma(z),\vartheta_S(z)),\vartheta_D)$. They reach their maximum after the transition into descent is completed at t_t; however, after transition time t_t, the theoretical position errors e_{x-y} and e_z (21) of improved model (3) are constant. The theoretical position errors e_{x-y} and e_z are presented in Fig. 4 for constant Mach number speed regime transition into the descent with standard constant angle of $\theta=3°$.

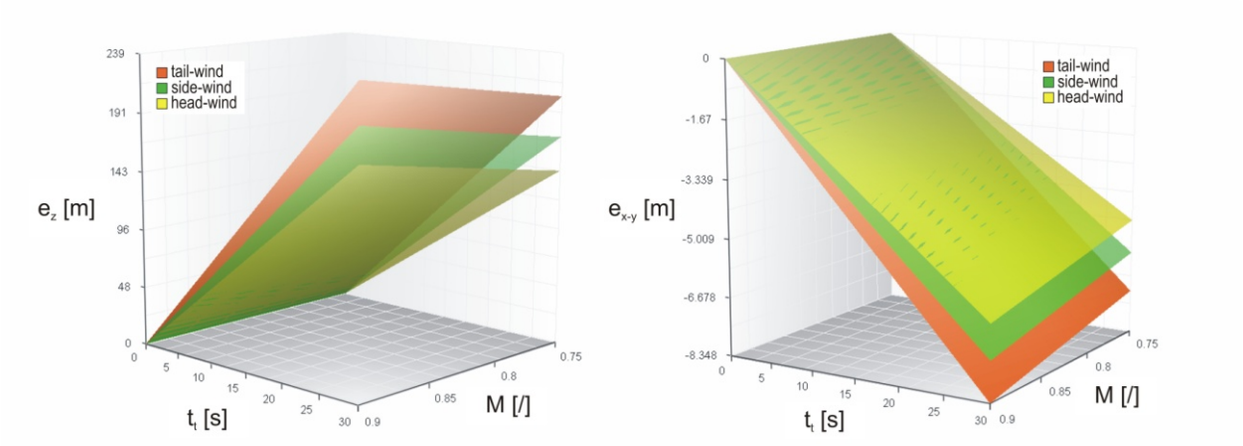

Figure 4. The improved model aircraft position errors in vertical e_z and horizontal $e_{x\text{-}y}$ plane after transition into descent.

While the horizontal plane $e_{x\text{-}y}$ theoretical position error of improved model (3) is negligible, the vertical plane e_z position error will be in the worst case almost equal to the reduced vertical separation minimum (RVSM) standard, in high–speed long–duration transition into descent, in tail–wind conditions (Fig. 4). However, as the vertical plane e_z position error is predictable and constant after transition into descent, the future aircraft descent trajectory is determinable and with corrections for the e_z, accurate as well.

3.2.2 Aircraft trajectory prediction errors

The descent trajectory prediction error of each model was determined by comparison of future trajectory predicted for the next 900 seconds (15 minutes) using each model (2) and (3) with the actual flight data recorded on commercial flight of Airbus A320 [10]. The ATC imposed break in actual flight which came after the TOD was used to foster trustworthiness of the methodology for the determination of the trajectory prediction error. The results of comparison are presented in Fig. 5, where point A indicates the TOD and B denotes the tropopause (ISA–1,24°C). At C the descent is interrupted, at D resumed, and at point E the descent speed regime has been altered from descent with the constant Mach number (0.78) to descent with the constant calibrated airspeed (280kt).

The trajectory prediction error of a primitive model of aircraft relative motion (2) clearly increases with the look-ahead time.The reason for such error is in the design of the primitive model of flight being ignorant to the variation of a true airspeed due to the static air temperature gradient in the troposphere. Within next 300 seconds (5 minutes) after the descent is resumed (at E), the trajectory prediction error of the primitive model exceeds 30% of the RVSM standard.

For the entire look-ahead time (15 minutes) of an aircraft future trajectory, predicted with the improved model of flight (3), its trajectory prediction error is stable in oscillations within ±16% of the RVSM standard. Being for the factor of at least 3 more accurate in trajectory prediction as the primitive model, the improved model promises greater reliability of conflict detection.

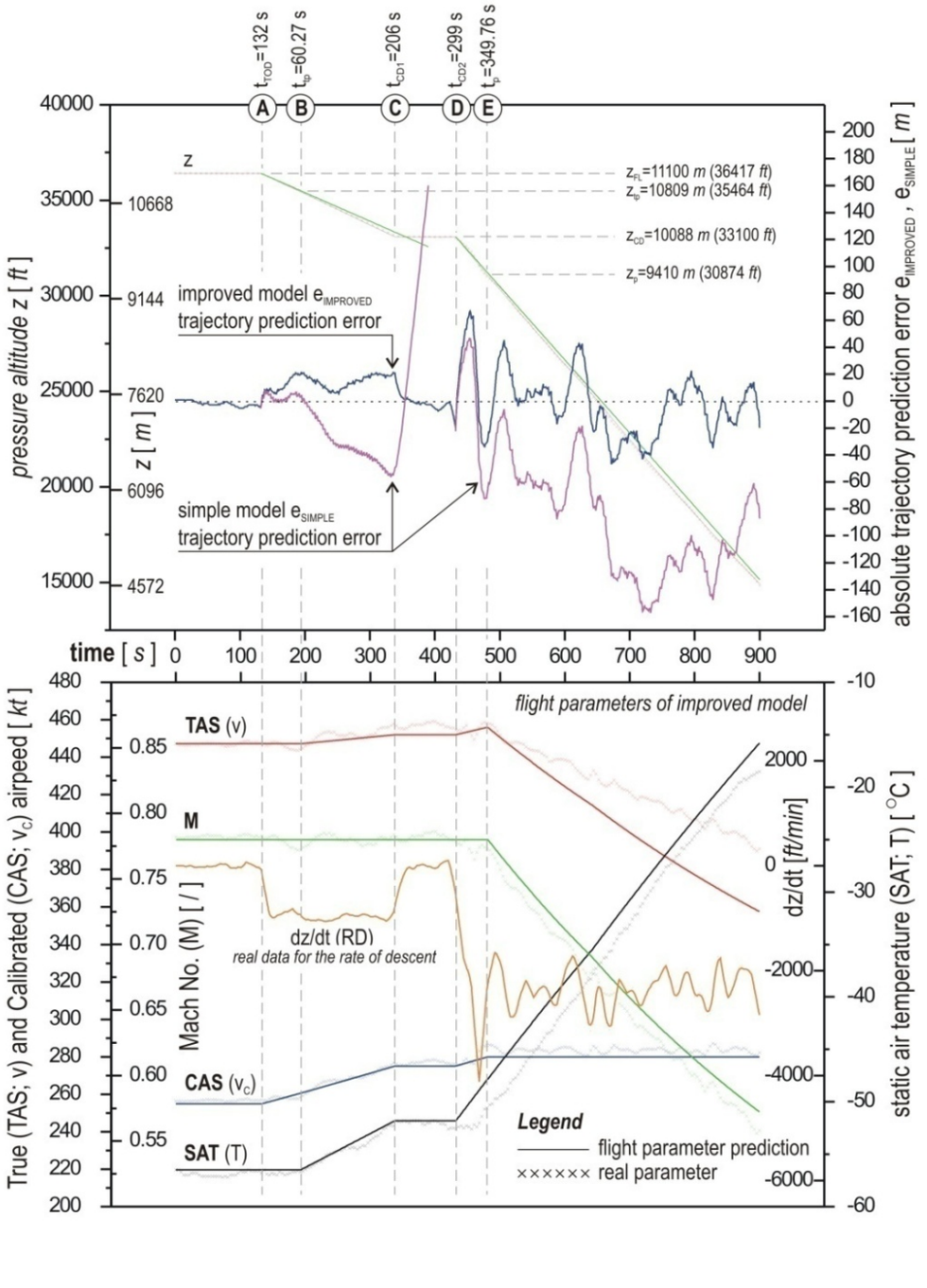

Figure 5. Trajectory prediction error of the primitive and improved model of flight compared to the flight data of real commercial flight.

3.2.3. Aircraft relative position error analysis

Initial separation $\mathbf{r}_{R.C}(\tau_{T/P},\psi_R)=\left(x_{R.C}(\tau_{T/P},\psi_R),y_{R.C}(\tau_{T/P},\psi_R),z_R(\tau_{T/P})\right)$ between aircraft A2 and A1 crossing at relative heading Ψ_R, is at the moment $\tau_{T/P}$ when A2 plans to initiate its descent at the TOD, critical (as shown in Fig. 6)if separation between them is lost after critical time t_C while A2 descents:

$$\underbrace{x_{R.C}\left(\tau_{T/P},\psi_R\right)+\int_0^{t_C}F_x(t)dt}_{x_R\left(t_C,\psi_R\right)}\le\left|r\right|+H\,\mathrm{tg}\,\theta_R(\sigma(h))$$

$$\underbrace{y_{R.C}\left(\tau_{T/P},\psi_R\right)+\int_0^{t_C}F_y(t)dt}_{y_R\left(t_C,\psi_R\right)}\le\left|r\right|+H\,\mathrm{tg}\,\theta_R(\sigma(h)) \qquad (22)$$

$$\underbrace{z_R\left(\tau_{T/P}\right)+\int_0^{t_C}F_z(t)dt}_{z_R\left(t_C\right)}\le\left|H\right|$$

where r is separation minimum in a horizontal plane, H is separation minimum in a vertical direction while time functions $F_x(t)$, $F_y(t)$, and $F_z(t)$ are defined either by primitive (2; PRIM) or advanced model (3-19; ADV) of aircraft relative motion.

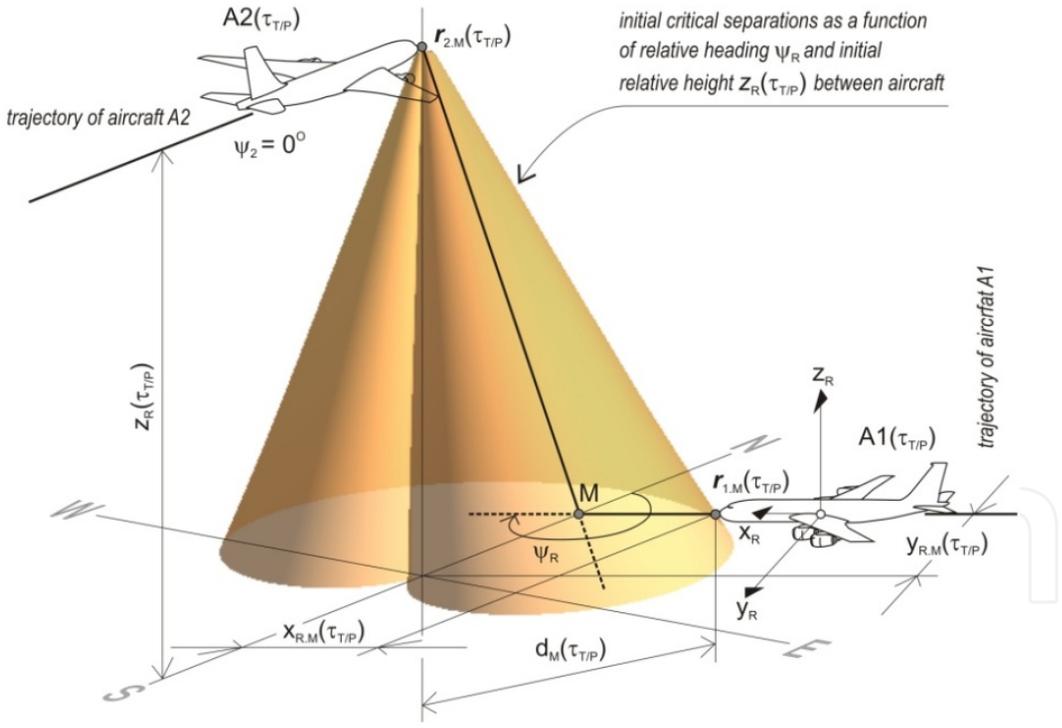

Figure 6. Critical initial separation between aircraft (collision in M is presented as special case of (22) where $r, H = 0$).

Figure 7 shows typical conflict detection error of the primitive model expressed with the error of relative distance between aircraft in close encounter situation in the horizontal plane ε_{dx} and ε_{dy} defined (according to (22) and Fig. 6) as:

$$\varepsilon_d\Big|_{z_R(\tau_{T/P})} = \Bigg[\underbrace{\left(x_{R.M}(\tau_{T/P},\psi_R)\Big|_{z_R(\tau_{T/P}):\mathrm{ADV}} - x_{R.M}(\tau_{T/P},\psi_R)\Big|_{z_R(\tau_{T/P}):\mathrm{PRIM}} \right)^2}_{\varepsilon_{dx}\Big|_{z_R(\tau_{T/P})}} + \underbrace{\left(y_{R.M}(\tau_{T/P},\psi_R)\Big|_{z_R(\tau_{T/P}):\mathrm{ADV}} - y_{R.M}(\tau_{T/P},\psi_R)\Big|_{z_R(\tau_{T/P}):\mathrm{PRIM}} \right)^2}_{\varepsilon_{dy}\Big|_{z_R(\tau_{T/P})}} \Bigg]^{\frac{1}{2}} \tag{23}$$

Imagine an aircraft A2 initiating the descent, then the vertical axis in Fig. 7 represent the relative height between A2 and intruder A1 below at the time of initiation of descent $z_R(\tau_{TOD})$. Note how fast the error with which the primitive model predicts future distance between aircraft in encounter incessantly increases after the descending aircraft starts to descent with the constant calibrated speed regime (after wasp-like contraction of a graph on Fig.7).

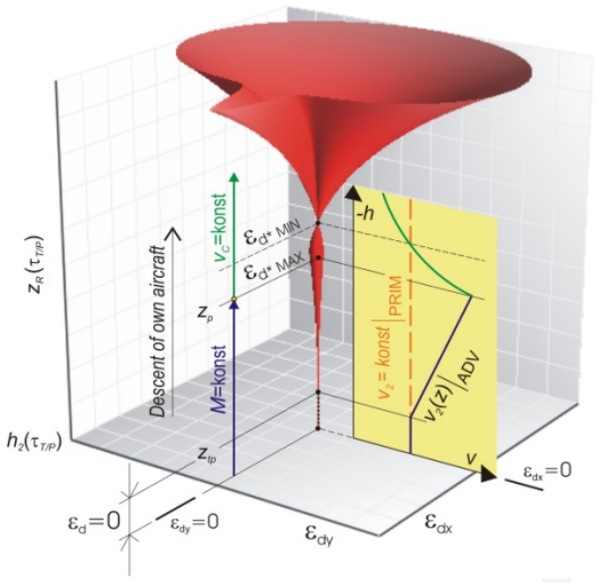

Figure 7. The relative distance between aircraft error of the primitive model of flight.

Investigation of the relative distance between aircraft error of the primitive model shows, as presented in Fig. 8, that the error ε_d will definitively (in any encounter situation) exceed r horizontal separation minimum (in Fig. 8 is represented by a cylinder). The peak values of relative distance between aircraft error ε_d are specific for head-on encounters ($140° < \psi_R < 220°$) and head winds relative to the descending aircraft A2 ($90° < \xi < 270°$; tail wind for the intruder A1). The error of relative distance between aircraft ε_d increases exponentially with the wind speed w (Fig. 8).Horizontal separation minimum $r$will be surpassed by relative

horizontal distance error ε_d(23) sooner at smaller initial relative height between intruder A1 and descending aircraft A2 (10000ft@75kts of wind) in windy atmosphere and when the descending aircraft is faster than intruder.

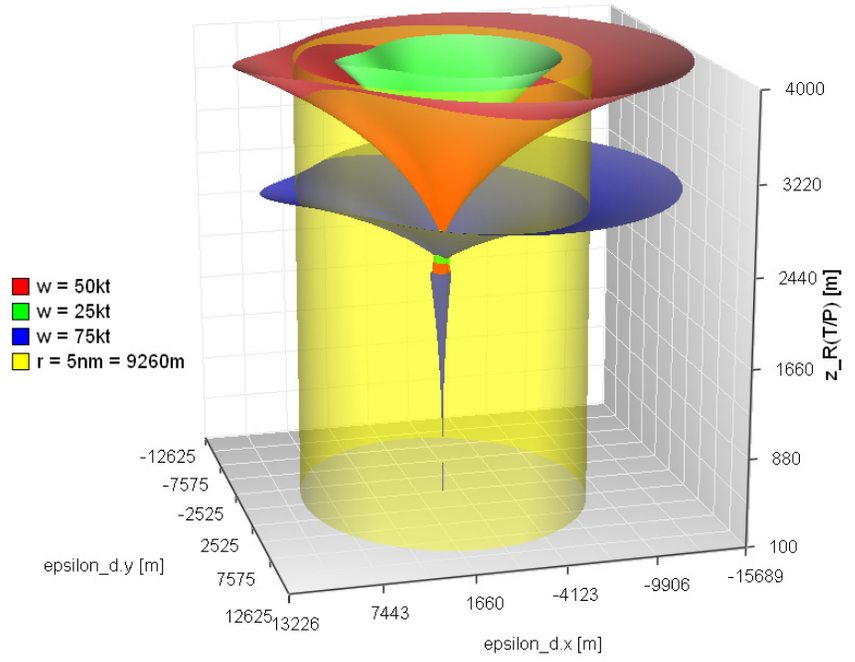

Figure 8. The relative distance between aircraft error of a primitive model exceeds the horizontal separation minimum.

Based on the critical initial separation between aircraft (22), the error of relative position between aircraft in the vertical direction ε_z depends upon the rate of descent and the speed regime change management of descending aircraft $dz(t)/dt\big|_2 = f(v_2(\sigma_2(z)),\vartheta_S(z)),\psi_2,\theta_2(\sigma_2(z)),\vartheta_D)$ (4) and is defined as:

$$\varepsilon_z = \left(\frac{z_R(\tau_{T/P})}{F_z(t)}\bigg|_{\text{ADV}} - \frac{z_R(\tau_{T/P})}{F_z(t)}\bigg|_{\text{PRIM}} \right) \frac{dz(t)}{dt}\bigg|_2 \tag{24}$$

The analysis of the primitive model error of relative position between aircraft in vertical direction ε_z (24) is shown in Fig. 9. As long as the true airspeed increases (Fig. 6) in constant Mach number descend (6-12), the primitive model (2) is *slow* in defining the future vertical separation between descending aircraft A2 and intruder A1 below. Descending aircraft A2 will actually fly lower than predicted, and the actual vertical separation between aircraft will be smaller than predicted. After the speed regime change, the true airspeed will decrease (Fig. 6) in constant indicated airspeed descent (13-19), consequently the primitive model (2) is *to fast* in defining the future vertical separation between aircraft. Descending aircraft A2 will actually fly higher than predicted, and the actual vertical separation between aircraft will be greater than predicted. It is the constant indicated airspeed descent phase where the relative position between aircraft in vertical direction ε_z (24) of the primitive model increases exponentially and exceeds the vertical separation minimum (Fig. 9).

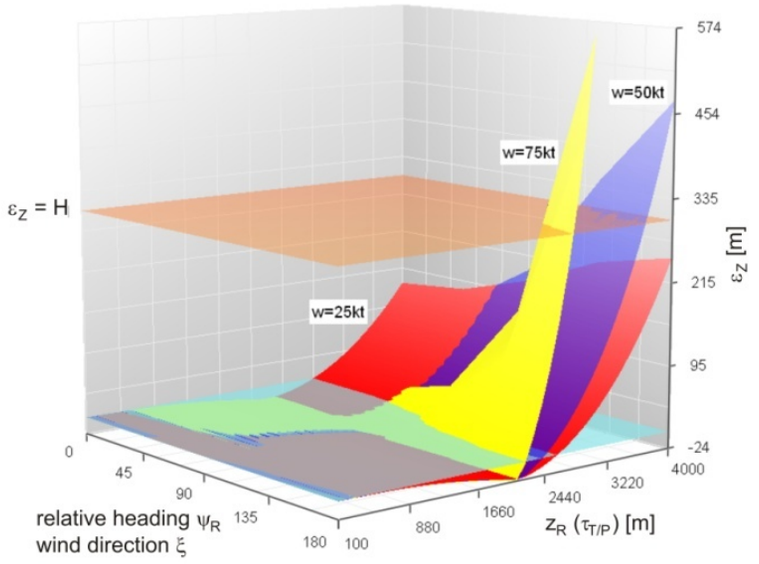

Figure 9. The primitive model error of relative position between aircraft in vertical direction (reduced vertical separation minimum is shown).

3.3. Reliability of conflict detection

The primitive model error of relative position between aircraft in vertical direction εz (24) will vary in a range of 10% of the RVSM standard for the conflict encounters up to 2000m (6500ft) below tropopause at moderate wind conditions (w = 26m/s (50kt)). However, after 5 minutes of descent and 3600m (12000ft) below tropopause, that is 70 km along the descent trajectory, the error of the primitive model will in vertical direction εzincrease to 170% of the RVSM standard (Fig. 9).

The consequence is that, even before the relative horizontal distance error exceeds the horizontal separation minimum, the primitive model of relative motion becomes blind and unable to detect threatening conflict between aircraft. At the same time conflict alerts of the primitive model will be false resulting in the unnecessary conflict avoidance maneuvering which will actually be unsafe since it can lead into the undetectable conflict with yet another aircraft (domino effect).

The inability to detect loss of separation and erroneous conflict detection of the primitive model of aircraft relative flight (2) is addressed in Fig. 10. From (22) the minimal and maximal initial critical separations that will result in the loss of separation are determined and shown in Fig. 10. Clearly both, the area of undetected conflicts and the area of false conflict detection of the primitive model increase with increasing initial vertical separation between aircraft $z_R(\tau_{T/P})$ at the planned initiation of descent. Those areas increase exponentially for head-on encounters in windy conditions and if descending aircraft flies slower than the intruder. In case of moderate wind the sum of the area of false conflict detection and the area of undetected conflicts will increase to approximately 50% of the area of correct conflict detection in head-on encounter at initial vertical separation of 3000m (6500ft) if descending aircraft is 20% slower than intruder.

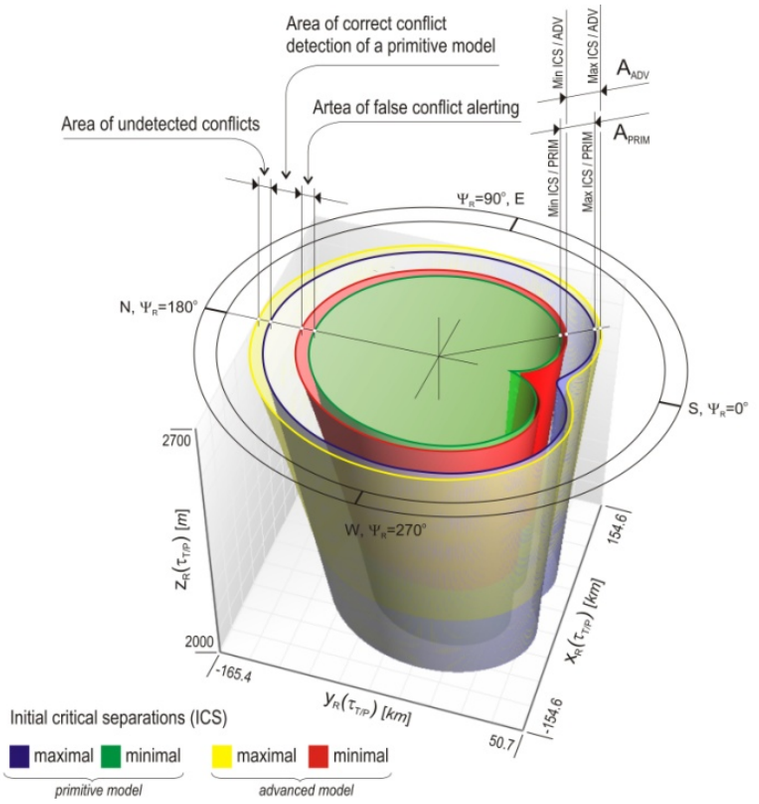

Figure 10. Inability of conflict detection and/or incorrect conflict detection of the primitive model in horizontal plane.

4. The infrastructure of autonomous flight

For the AASAS on-board aircraft to be based on the improved model of the aircraft relative motion (3) numerous information ofeach aircraft flight in the conflict detection zone has to be exchanged via Automatic Dependence Surveillance–Broadcast (ADS–B) as shown in Fig 11.

According to the improved model of the aircraft relative motion (3) those information (Fig. 11) are:

a. instantaneous flight parameters ζ_I: aircraft position, heading, speed regime and rate of climb or descent,
b. flight plan – i.e. future intentζ_P: set of each future navigational fix in place and time with corresponding flight parameter which will be altered at the fix, and
c. real time data on static ϑ_S (static air temperature at the atmospheric reference level) and dynamic ϑ_D state (wind speed and direction) of atmosphere (Fig. 12).

Since the trajectory prediction error pattern of the improved model of aircraft relative motion is non-increasing and stable with the absolute error less than the RVSM standard (Fig. 5), the AASAS on-board each aircraft will be, based on information exchanged, able to predict stable future four-dimensional traffic situation in the conflict detection zone around aircraft. In case of threatening conflict of separation loss the AASAS willaccurately define

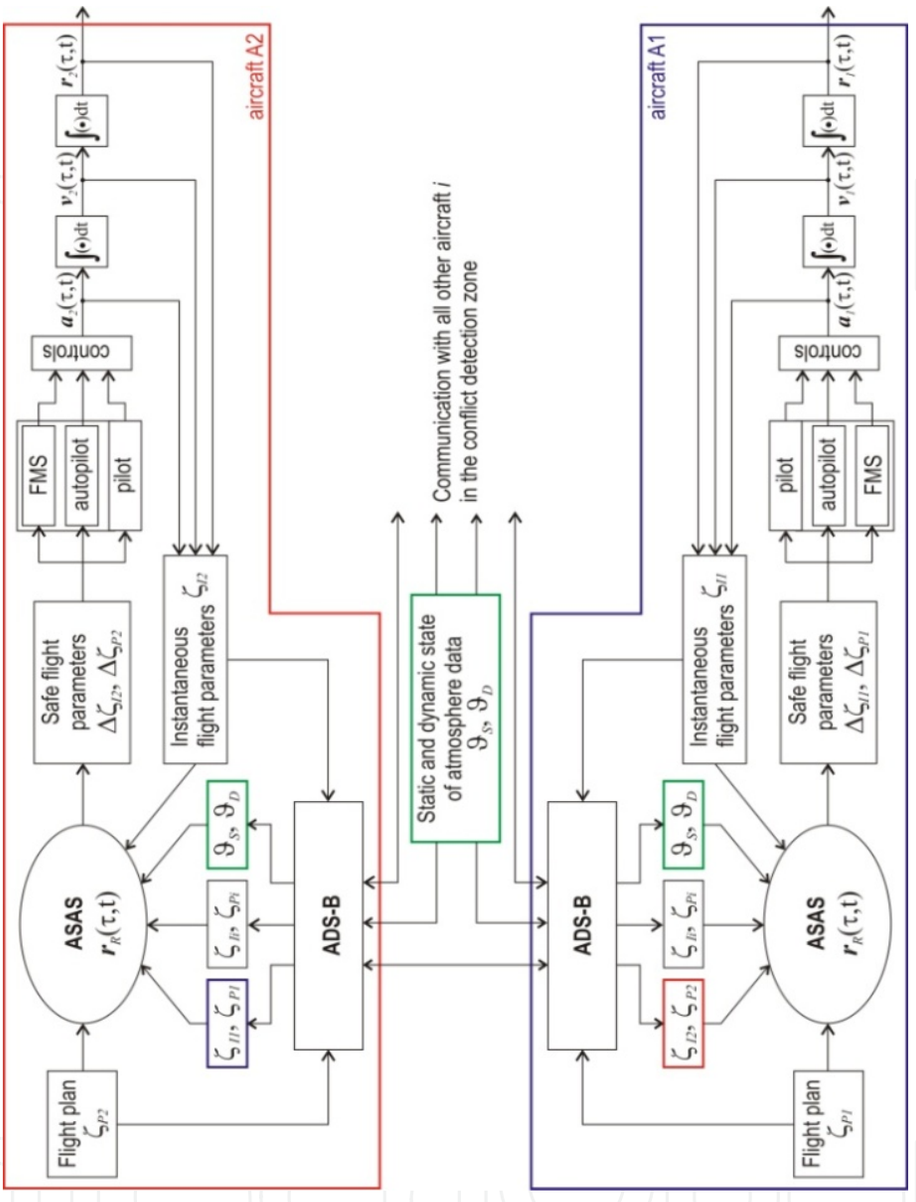

Figure 11. Information exchange requirements of the improved model of flight based Airborne Separation Assurance System.

the safe parameters$\Delta\zeta_I$ and $\Delta\zeta_P$ of conflict avoidance maneuveringfor the execution by the FMS/ autopilot or crew.

Investigation of the relative distance between aircraft error of the improved model as well as its trajectory prediction error revealed (Fig. 5), that the temperature at the atmospheric reference level is the improved model of aircraft relative motion accuracy most critical parameter. The necessary data on atmospheric conditions defined by (3) and their proposed format for up-link to the aircraft are presented in Fig. 12 and obtainable by the Mode-S transponder (for example).

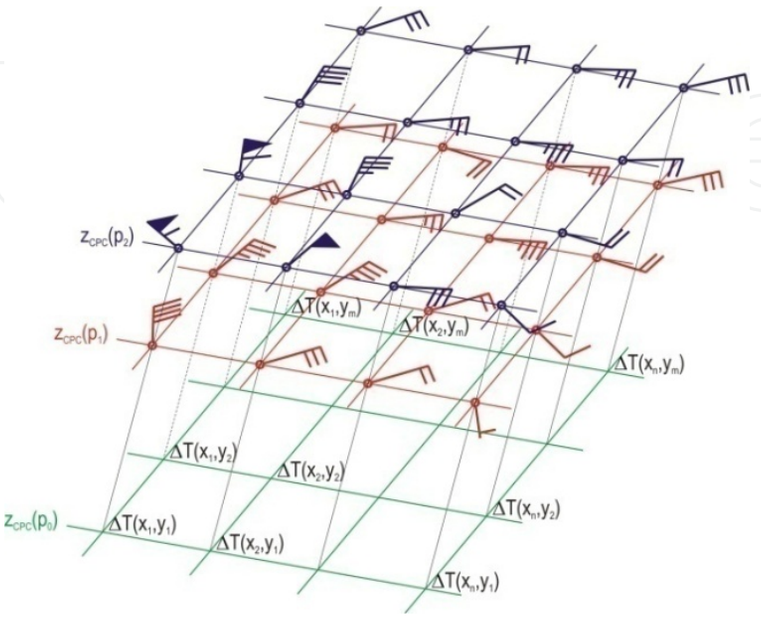

Figure 12. Proposed format of atmospheric conditions data available to each airborne aircraft.

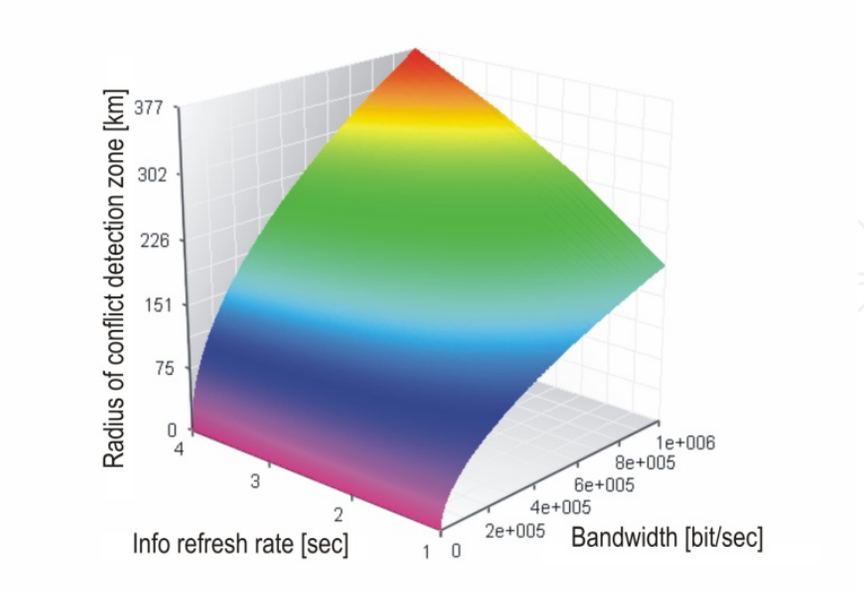

Figure 13. The feasible radius of conflict detection zone of the improved model of aircraft relative motion based ASAS.

The quantum of necessary information which has to be continuously and uninterruptedly exchanged between each aircraft aloft within radius of conflict detection zone of each other and with the ground systems providing them atmospheric conditions data impose concerns about ADS–B ability to exchange all those information. However, based on the assumption that the complete uncompressed data necessary comprise 1150 bits (comparison [6]) of exchanged massage among 30 aircraft per 100×100nautical miles (0.000875 aircraft per square km (Eurocontrol Performance Review Report 1999-2010)) on each of 28 flight levels from FL410 to FL150 (exaggerated aircraft density), and Universal Access Transceiver with the bandwidth of 1Mbit/s [6] is used, then the conflict detection zone with radius of up to 370 km (200 nautical miles) can be realized with the complete information refresh rate of 4 seconds. Relationships described and influence of information refresh rate and the data exchange bandwidth on the feasible radius of conflict detection zone are presented in Fig. 13.

5. Conclusion

Notwithstanding its many–sided complexity, the introduction of the AFA is inevitable, as ideas of unmanned cargo and passenger aircraft are emerging and the first UASs are already inexorably taken to the skies. The AFA technology development is applicable to the coming generation of aircraft and ATM systems with increasing automation anticipated to cope with increasing demand for airspace capacity.

Imminent increase in conflict encounter threatening aircraft transitioning to and from the AFA can be dispersed along the entire trajectory of aircraft with reduced severity of each remaining area of increase in conflicts with the introduction of descending or climbing transitions and AA reception/dispatch zone below the AFA where expected aircraft mix can be handled. The enabling technology is machine–based decision–making airborne AASAS and ground–based automation ASAS communicating by data–link. This AASAS should be capable of accurate conflict detection before descending aircraft exits the AFA or before ascending aircraft enters AFA. Otherwise the conflict encounters (loss of separation between aircraft) imminent in the AA Reception/Dispatch Zone of Fig. 1 are unavoidable.

The investigation of trajectory prediction error of a primitive model of aircraft relative motion clearly indicates the reason for the unstable prediction of future three-dimensional airborne traffic situation with existing (TCAS-like) technology and methodology. Furthermore, the conclusion can be drawn from the study that conflict detection and resolution is not safe and actually impossible for look-ahead time longer than 5 minutes in the airspace where aircraft are flying their trajectories in the vertical plane. Consequently, the primitive model of aircraft relative motion based airborne separation assurance cannot assure promptly and accurate conflict detection and therefore cannotfacilitate the AFA introduction.

The improved model of aircraft relative motion compared to its primitive pendant appears promising particularly because of the stability of its trajectory prediction error. This error

might be less than described in the paper if the real reference atmospheric temperature is provided to the AASAS on-board each aircraft.

Plain proof is provided that the AFA and autonomous flight operations are feasible and basic–level AFA operational procedures are introduced. Crucial to the AFA introduction feasibility are technologies enabling: (a) sufficient bandwidth for reliable data–link communications, (b) capability to predict accurate and stable future 4D traffic situations with sufficient look–ahead time, (c) multi–factor analyses for real–time determination of safe transitioning trajectory including determination of the TOD, TC, and AA reception/dispatch zone collector airway selection, (d) adaptive airways structuring of AA, and (e) dynamic airspace sectorization.

Author details

Tone Magister and Franc Željko Županič
SLOVENIA CONTROL, Slovenian Air Navigation Services, Ltd, Ljubljana, Slovenia

Acknowledgement

The author is sincerely grateful to Cpt. Aleksander Sekirnik of Adria Airways for his unselfish support, advice and help.

6. References

[1] ACARE: "The Challenge of Security", in Strategic Research Agenda 1, Vol. 2, Advisory Council For Aeronautics Research in Europe, 2002.
[2] Beers, C.,Huisman, H.: "Transitions between free flight and managed airspace", 4th USA/Europe ATM R&D Seminar, Santa Fe, NM, USA, 2001.
[3] Bilimoria, K., Lee, H.: "Performance of air Traffic Conflicts for Free and Structured Routing", AIAA Guidance, Navigation, and Control Conference, Paper No. 2001- 4051, Montréal, Canada, 2001.
[4] Duong, V., *et al*, "Sector–Less Air Traffic Management," *5th USA/Europe ATM R&D Conf.*, Budapest, Hungary, 2003.
[5] Erzberger, H.: "The Automated Airspace Concept", 4th USA/Europe ATM R&D Seminar, Santa Fe, NM, USA, 2001.
[6] Hoekstra, J.M.: Designing for Safety – The Free Flight Air Traffic Management Concept, Ph.D. thesis, Technische Universiteit, Delft, The Netherlands, 2001.
[7] Kopardekar, P., Magyarits, S.: "Measurement and Prediction of Dynamic Density", 5th USA/Europe ATM R&D Seminar, Budapest, Hungary, 2003.
[8] Magister, T.: "The problem of mini-unmanned aerial vehicle non-segregated flight operations", *Traffic*, 2007, vol. 19, no. 6, pg. 381-386.
[9] Magister, T.: "Transition flight between the autonomous flight airspace and automated airspace", *Traffic*, 2008, vol. 20, no. 4, pg. 215-221.

[10] Magister, T.: "Long range aircraft trajectory prediction", *Traffic*, 2009, vol. 21, no. 5, pg. 311-318.

[11] Mondolini, S., Liang, D.: "Airspace Fractal Dimensions and Applications", 3th USA/Europe ATM R&D Seminar, Napoli, Italy, 2000.

IntechOpen